# Ru/$Al_2O_3$ CATALYST-ASSISTED PROCESSING OF WASTE SILANE-GRAFTED CROSS-LINKED POLYETHYLENE

***Pavel Straka*, Olga Bičáková, Jaroslav Cihlář***

*Institute of Rock Structure and Mechanics, v.v.i., Czech Academy of Sciences,*
*V Holešovičkách 94/41, 18209 Praha 8, Czech Republic,* straka@irsm.cas.cz

*Waste crosslinked polyethylene (XLPE) can be a source of valuable hydrocarbons for further use. XLPE is widely used material which – unlike polyethylene – is very stable both chemically and mechanically. Therefore, its waste is difficult to process. A very promising way is slow pyrolysis catalyzed by ruthenium (Ru/$Al_2O_3$) which allows the conversion of waste into hydrocarbons via degradation of rigid chemical structure of cross-linked material. High hydrocarbon yields (91–92 wt.%) were achieved by slow pyrolysis without or with catalyst, but significant changes in the composition of resulting gas and oil were found with the Ru/$Al_2O_3$ catalyst. To reveal the possibilities of using this catalyst for processing of XLPE at a relatively lower final temperature (max. 480 °C, mostly 450–470 °C), an effect of the catalyst on degradation of XLPE structure and related rheological properties of XLPE melt was investigated. It was found that the activation energy of degradation decreases significantly in the presence of the catalyst and the degradation is greatly facilitated by Ru/$Al_2O_3$ at the defect sites of the XLPE structure (the tertiary carbons). By the catalyst, the torque for XLPE melt and the its shear viscosity are significantly reduced already at 250 °C. Thus, Ru/$Al_2O_3$ catalyst, even in very small amounts (1 wt.% Ru), significantly promotes the degradation of XLPE structure and reduces the solid pyrolysis residue. This finding greatly facilitates the processing of waste XLPE. The catalytic mechanism of action of Ru is outlined and the equations for the XLPE cleavage are given. The main product of processing, pyrolysis oil, can be used as a clean heating fuel, or oil for further use, or a source of solvents, liquid and solid hydrocarbons, especially paraffin.*

*Keywords: pyrolysis, ruthenium; polyethylene; catalyst*

Došlo 7/1/2026, přijato 29/3/2026

## 1. Introduction

Because of its unique properties and stability, cross-linked polyethylene (XLPE) is used extensively for the manufacture of pressure pipes for the installations of water-, chlorinated water- and steam-distribution systems, thermal equipment in industrial plants and households, and also for underfloor heating. It is also utilized for the insulation of electrical conductors [1]. The wide range of applications is reflected in the amount of production and installation waste to be removed from the environment. Unfortunately, the disposal of this waste now consists mainly of incineration and landfilling, which are neither appropriate nor efficient ways of disposing of this precious-material waste. Therefore, it must be processed [1], preferably into products with a high utility value.

XLPE has exceptional mechanical properties as well as very good chemical and solvent resistance, so, its reprocessing, recycling and modification remain difficult. Moreover, waste XLPE is not of technological nature, which means that it cannot be returned to the production process, because XLPE product quality requirements are too high and could not be met if waste XLPE was used as feedstock. Due to this, it is necessary to find an appropriate method of processing, which is not only realistic, but also provides useful products [2]. Such a method appears to be slow pyrolysis at a final temperature below 500 °C catalyzed by ruthenium.

The low-temperature pyrolysis of waste XLPE is rarely addressed in available scientific and professional journals [3,4,5], which rather focus on the description of structure of polymer material and problems of degradation of virgin polymers, mechanisms of scission of polymer chains and polymer networks [6]. Recently a high-temperature $CO_2$ assisted gasification of XLPE waste with focus on the kinetics and syngas yield and properties was investigated [7]. On the other hand, the catalytic function of ruthenium has been intensively studied in recent years.

Generally, ruthenium catalysts exhibit high activity and selectivity and are often resistant to sulfur and other impurities. They are very useful for oxidative transformations (epoxidation of alkenes, formation of dioxygen species, dihydroxylation of olefins and oxidative dehydrogenation of alcohols) [8], further, for reducing carbonyls to alcohols and aromatics to cyclohexanes, the selective reduction of 1-alkenes to alkanes and nitriles to amides and dehydrogenation of alcohols to aldehydes or ketones [9]. Further, ruthenium complexes have specific advantages in hydroformylation [10] and, finally, ruthenium catalyst is very useful for methanation of CO/$CO_2$ [11]. The scission function of ruthenium has been intensively studied in recent years and the results suggest that it can be suitable for this purpose [12–15]. Rorrer et al. (2021) report that the cleavage of strong C-C bonds in polyolefins can be performed using ruthenium and hydrogen via hydrogenolysis mechanism [16].

As far as conventional polyethylene (PE) is concerned, Huang et al. [17] used combination Ir-

DOI: 10.35933/paliva.2026.01.01

complex/$Al_2O_3$ and $Ru_2O_7/Al_2O_3$ catalysts and demonstrated for the first time Ir-Ru efficiency in the quantitative conversion of PE to a mixture of alkanes. Conversion of 120 mg PE with hexane to oil and wax products after heating for 3 days at 150 °C yielded 56–98% oil with alkanes and 2–44% wax with alkanes. Based on this work, the work of Brookhart et al. [18] and other findings [19,20], Farkas et al. [21] used Ru-catalysts for recycling of PE. The authors processed PE in two stages to the resulting polypropylene. In the first stage, slow pyrolysis yielded oil containing long-chain olefins, and in the second stage they used two ruthenium complex catalysts to split the oil in an ethylene atmosphere to produce the resulting polypropylene. The authors report that 75 g of propylene can be obtained from 100 g of waste PE and 45 g of ethylene. Overall, ruthenium can be used for the decomposition of XLPE, but the pyrolysis conditions must be well defined, and the ruthenium catalyst must be readily available.

It must be emphasized that there is a big difference between pyrolysis of polyethylene (whether LDPE, or medium density polyethylene, or HDPE) and cross-linked polyethylene. Due to its extraordinary chemical and mechanical stability [22–26], great attention must be paid to pyrolysis conditions. Their importance comes to the fore especially when processing waste XLPE on a large scale, as they reduce the temperature of the onset of decomposition, increase the efficiency of the process and enable a deeper degradation of XLPE structure.

Among the catalysts most often used for decomposition of polyethylenes and other plastics [27,28], the following were considered for the decomposition of waste XLPE. Amorphous and mesoporous $SiO_2/Al_2O_3$ [29,30], MCM with $Al_2O_3$ [31], ZSM-5 zeolite [32,33], FCC [34], activated carbon [35] and faujasite (zeolite Y) [36]. These catalysts certainly work for various polyethylenes and blends thereof, but higher amounts of waxy compounds and lower liquid yields are obtained. Therefore, a different approach is required for XLPE waste. The cause is in the undefined impurities and especially in the rigid structure of XLPE. Another problem is that the mass balance and efficiency of process are not evaluated.

Therefore, this work investigates the effect of Ru/$Al_2O_3$ catalyst on waste XLPE degradation based on its behavior during pyrolysis without and with catalyst, kinetics of the process, the rheological properties of melt of material alone and with catalyst, analysis of pyrolysis products and estimation of the process conditions.

## 2. Materials and methods

### 2.1. Materials

The waste used was colored silane-grafted XLPE flakes of a few mm up to 1 cm in size, resulting mainly from the production of XLPE pressure tubes, hot water pipes and cable insulation. The waste was obtained from Central Bohemian producer in quantities of several tens of kg. It was homogenized, then samples of 20 g, 50 g and 100 g were taken for analyses, rheological measurements and pyrolysis experiments, resp. Waste used contained little water (0.09 wt.%) and ash (0.66 wt.%), and a high percentage of combustible matter (99.25 wt.%). The degree of crosslink of the XLPE used was 65% according to DIN 16892 and ASTM Standard F876, the Si content was of 0.05 wt.%. Lower and higher heating values of this waste material were LHV of 42.89 MJ $kg^{-1}$ and HHV of 45.97 MJ $kg^{-1}$.

As catalyst, ruthenium dispersed on a porous $Al_2O_3$ matrix was used, while loading of Ru was of 5 wt.% (Merck Sigma-Aldrich CZ, s.r.o., powder (< 0.15 mm) with moisture content < 2 wt.%).

### 2.2. Methods

*TG/DSC method.* Behavior of waste XLPE alone and with Ru/$Al_2O_3$ catalyst during pyrolysis was investigated by the thermogravimetric method (TG) on a Setaram Setsys Evolution 18 analyzer. About 20 mg of XLPE sample or 16 mg of XLPE with 4 mg of catalyst was heated at the rates of 5–20 K $min^{-1}$ in the temperature range of ~25–550 °C in an inert atmosphere He at the flow rate of 20 $cm^3$ $min^{-1}$. Simultaneously, differential scanning calorimetry (DSC) curves were recorded to determine the melting point and decomposition temperatures. From the TG and DSC data obtained, the dependences of both overall activation energy and the frequency factor on the reaction progress were calculated using the AKTS Thermokinetics software, version 2.32. The Friedman differential isoconversional kinetic method was applied, while heating rates 5, 10, 15, and 20 K $min^{-1}$ were used.

*Rheological properties.* The effect of catalyst on the scission of the XLPE structure was also determined using the plastographic method and measurements of the shear viscosity of melt at 250 °C. The effectiveness of catalyst was tested by changing the torque during the kneading of 50 g of XLPE with 5 or 10 g of catalyst on a Brabender PLE 651 plastograph equipped with a W 50 EHT measuring mixer. The chamber temperature was of 250 °C, the rotor-rotation speed of 120 per min, the chamber-beam load was 10 kg; materials were always kneaded for 40 min. The results were the time dependences of torque for material alone and material with catalyst. After kneading, an obtained material was cooled to laboratory temperature, crushed on a knife mill and fed into a rheometer. The viscosity of this material was then measured with a RH 2000 high-pressure capillary rheometer (Malvern Instruments, Inc.) at 250 °C. Thus, these measurements provided the flow curves at 250 °C.

*Pyrolysis.* Pyrolysis up to 480 °C was performed with waste silane-grafted XLPE, both with and without catalyst. A pyrolysis unit (quartz reactor with electric heating, cooling system, gas holder, continuous sensing of temperature field and gas pressure and volume) enabling capture of all products was used [15]. Feedstock and catalyst weights were 100 g and 20 g, resp., while the powdered catalyst was placed in a layer above the sample, so that it does not mix with feedstock. The heating rate was always of 5 K $min^{-1}$, final temperatures were

450–480 °C, and the delay at the final temperature was of 30 min. Each pyrolysis run to a given final temperature was carried out three times. The relative standard deviation of the oil yield was 1–2 %, that of the solid carbonaceous residue yield was 4–5 % and that of the pyrolysis gas yield was 1–2 %.

The total gas obtained was analyzed on two Agilent Technologies 6890N gas chromatographs with three capillary columns 30 m × 0.32 mm while the analysis of $O_2$, $N_2$ and CO was performed on an HP-MOLSIV (40 °C) with carrier gas He (5 $cm^3$ $min^{-1}$) using TCD; $CH_4$ and $C_2$–$C_5$ hydrocarbons on a GS-Gaspro (60 °C) with carrier gas $N_2$ (20 $cm^3$ $min^{-1}$) using FID; $CO_2$ on a GS-Gaspro (40 °C) with carrier gas He (5 $cm^3$ $min^{-1}$) using TCD; $H_2$ on an HP-5 (40 °C) with carrier gas $N_2$ (7 $cm^3$ $min^{-1}$) using TCD. The relative standard deviations of individual gas component determinations were 1–3% ($n = 6$).

Oil components were identified on an Agilent Technologies 6890 chromatograph with an MSD 5975 mass spectrometer and a DB XLB (30 m × 0.25 mm) capillary column. The column was maintained at 50 °C for the first min, then the temperature was increased from 50 to 300 °C at the heating rate of 10 K $min^{-1}$; the column was then maintained at 300 °C for 6 min. The carrier gas was helium.

Analysis of Si in the starting XLPE and solid carbonaceous residue was performed by X-ray fluorescence method on a Spectro IQ, Kleve, Germany. The test samples were prepared by the pressed pellet method, where 4.0 g of material with a particle size of 15–20 µm was mixed with 0.9 g of binder (HWC Hoechst wax, Germany) for 10 min and pressed with a pressing force of 80 kN. Measurements were performed on the spectrometer with target Pd-material while the target angle from central ray was 90°. The focal point was a 1 mm × 1 mm square, the maximum anode dissipation was of 50 W with forced-air cooling (16.28 $m^3$ $min^{-1}$). The instrument used was equipped with a HOPG Barkla crystal.

## 3. Results and Discussion

To describe the effect of Ru/$Al_2O_3$ catalyst on the decomposition of waste XLPE, the TG/DSC method was firstly used, enabling the determination of melting and decomposition temperatures and the overall activation energy of decomposition.

### 3.1. Basic thermal phenomena of XLPE decomposition

In all cases, two important temperature intervals with significant heat flows were registered: 80–150 °C with maximum at 128–131 °C and 400–550 °C with maximum at 473–499 °C as DSC curves proved. In the first interval, melting of material occurs, in the second one, the total decomposition of crosslinked structure is in progress. DSC curves obtained are shown in Fig. 1 and described in Table 1. Regarding TG determination, for heating rates of 5, 10, 15 and 20 K $min^{-1}$, typical TG curves were obtained both without and with catalyst; the similar curves were obtained at decomposition of XLPE from cables with heating rate of 40 K $min^{-1}$ [37]. In all cases, conversion was completed at a temperature of 510–550 °C.

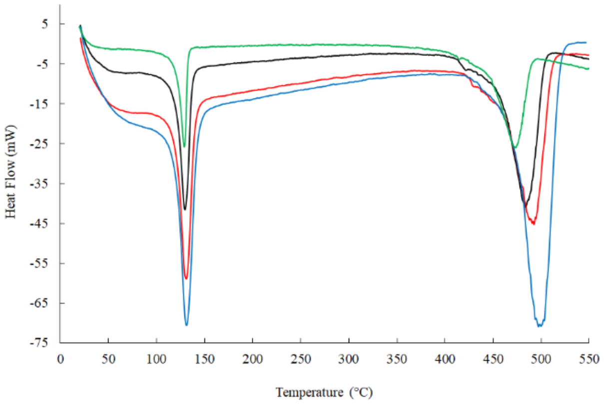

**Fig. 1a** DSC curves of waste XLPE at heating rates of 5 (green), 10 (black), 15 (red) and 20 (blue) K $min^{-1}$

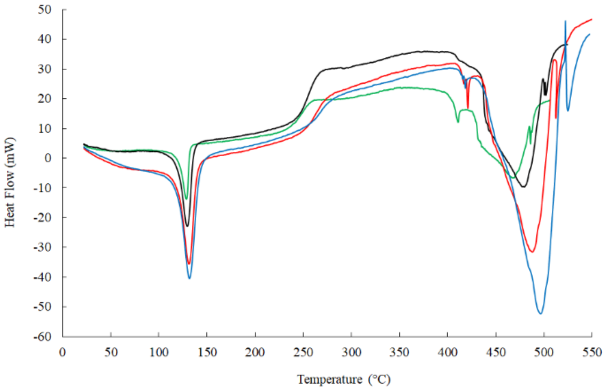

**Fig. 1b** DSC curves of waste XLPE with Ru/$Al_2O_3$ catalyst at heating rates of 5 (green), 10 (black), 15 (red) and 20 (blue) K $min^{-1}$

**Tab. 1** Heat phenomena at different heating rates ($w$). $T_{melt}$ – peak temperature of melting, $T_{endo}$ – peak temperature of decomposition ($n = 5$)

| Sample | $w$ (K $min^{-1}$) | $T_{melt}$ (°C) | $T_{endo}$ (°C) |
|---|---|---|---|
| Waste XLPE | 5 | 128.2 ± 0.5 | 472.8 ± 2.4 |
| | 10 | 129.0 ± 0.8 | 481.7 ± 2.7 |
| | 15 | 130.1 ± 0.8 | 491.8 ± 0.5 |
| | 20 | 130.7 ± 0.4 | 498.7 ± 1.6 |
| Waste XLPE + Ru/$Al_2O_3$ | 5 | 128.6 ± 0.5 | 468.0 ± 2.3 |
| | 10 | 129.5 ± 0.9 | 479.1 ± 2.6 |
| | 15 | 131.1 ± 0.9 | 488.3 ± 1.0 |
| | 20 | 131.7 ± 0.5 | 496.8 ± 1.5 |

As follows from Fig.1 and Table 1, decomposition of XLPE is preceded by melting. To assess the effect of catalyst on the process, it is therefore necessary to follow both its effect on melting and decomposition. As the activation energy of decomposition is the key item of the catalyst action, attention was paid to it first.

### 3.2. Activation energy of XLPE decomposition

The activation energy of waste XLPE decomposition ($E_a$) was determined and compared with that in the presence of Ru/$Al_2O_3$ catalyst. TG and DSC methods were used, while heating rates were 5, 10, 15 and 20 K $min^{-1}$. To determine the effect of catalyst used, $E_a$ of decomposition of waste XLPE alone and that with catalyst and their dependence on the reaction progress ($\alpha$) were calculated. As decomposition of waste XLPE is an Arrhenius-type process (the linear dependences ln $k$ on $1/T$, while $k$ is a rate constant and $T$ is a thermodynamic temperature, was always found), the Friedman differential isoconversional method could be applied [38]. The results are shown in Figs. 2 and 3. As expected, it was found that $E_a$ of decomposition was lower with catalyst than without it (Fig. 2, calculated from TG data, Fig. 3, calculated from DSC data).

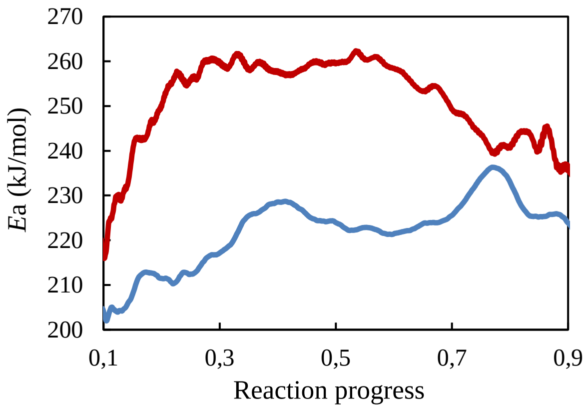

**Fig. 2.** Activation energy of decomposition of waste XLPE calculated from TG data for $\alpha = 0.1–0.9$. Red (upper) line – without catalyst, blue (bottom) line – with catalyst (1 wt.% Ru)

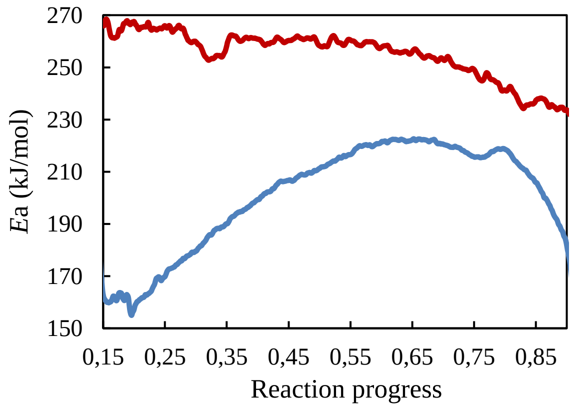

**Fig. 3**. Activation energy of decomposition of waste XLPE calculated from DSC data for $\alpha = 0.15–0.9$. Red (upper) line – without catalyst, blue (bottom) line – with catalyst (1 wt.% Ru)

Without catalyst, the formation of free radicals is initiated only thermally, but with catalyst, the bonds are split also by the action of Ru/$Al_2O_3$. Under such reaction conditions, different bond splitting reactions occur. It is significant that the curves obtained for decomposition without catalyst (red lines) are very different from those obtained with the catalyst (1 wt.% Ru, blue lines).

As follows from Fig. 2, in stages of decomposition $\alpha$ 0.1–0.9, $E_a$ is significantly lower with the catalyst compared to without it. It can be deduced that the basic factor of decomposition is temperature, but the catalyst used promotes the decomposition significantly.

Similar, though not the same, conclusions can be drawn from DSC data (Fig. 3). In the decomposition stages $\alpha$ 0.15–0.90, significantly higher $E_a$ values were recorded during decomposition without catalyst (red upper line in the figure) compared with it (blue bottom line in the figure). While without catalyst $E_a$ did not change much, from 268 to 232 kJ/mol, with catalyst this parameter changed significantly, from 155 to 222 kJ/mol. From $\alpha$ 0.2 to a flat maximum at $\alpha$ 0.6–0.7, $E_a$ increases as the blue bottom line in Fig. 3 shows, which can be explained by the deeper cleavage of crosslinked structure in the presence of catalyst compared to the cleavage without it. As $E_a$ is always lower in the presence of catalyst compared without it, it can be deduced that the thermal scission is supported by the catalyst used which at the same time enables a deeper splitting and depolymerization of XLPE structure. Scission is likely to be facilitated at defect sites in the XLPE structure, particularly at the tertiary carbons in the main chain where cross-link branching occurs (see equations 1 and 2 below). So, the effect of catalyst must be reflected in the composition of pyrolysis products. This conclusion is further confirmed below, see section 3.4.

### 3.3. Rheological properties of XLPE melt

As mentioned above, decomposition of XLPE is preceded by melting. Therefore, the properties of waste XLPE melt were further investigated to determine if and how the catalyst affects its behavior. To clarify this question, rheological properties of XLPE melt were tested. The basis is that scission is facilitated at defect sites of XLPE structure, especially at tertiary carbons in branching of main chain and crosslinks. This should be supported by catalyst while the degree of scission is reflected in the change in the rheological properties of melt. So, rheological properties of melt without and with catalyst should be different.

The effect of Ru/$Al_2O_3$ catalyst on the XLPE melt was tested by two methods: (a) measuring the torque during the kneading of waste XLPE while XLPE mass was of 50 g and initial temperature setting was of 250 °C; and (b) determination of shear viscosity of resulting melt after kneading as a function of the shear rate at 250 °C. The results obtained by torque measurements are shown in Fig. 4.

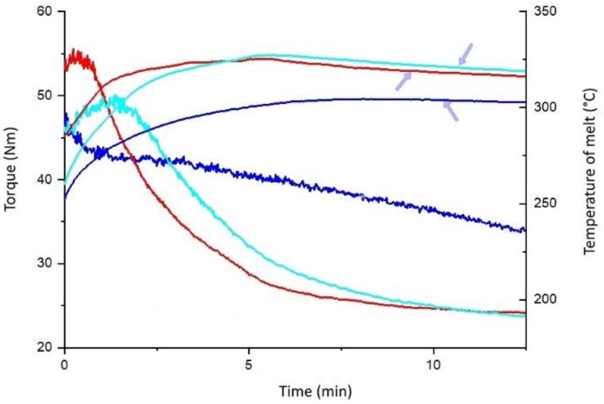

**Fig. 4.** Time dependence of the torque during kneading of waste XLPE recorded on the plastograph. Blue line – XLPE alone; turquoise line – XLPE feed with 0.5 wt.% Ru; red line – XLPE feed with 1 wt.% Ru. For temperature courses see the upper flat lines marked with arrows.

It is evident from the time course of torque that an addition of Ru/$Al_2O_3$ catalyst led to the rapid change of the XLPE structure, which was reflected in a sharp decrease of torque after induction period (first 2 min) at the initial kneading stage (~3.5 min) (turquoise and red lines compared to blue line). The effect of catalyst is thus significant, as the changes with catalyst occurs at relatively low temperatures and to a considerable extent, unlike XLPE changes without catalyst. (Note: A sharp decrease in torque was found with the addition of catalyst compared to without catalyst, even though the addition of catalyst implied the presence of solid particles and thus an increase in the average density of the sample. However, this is only possible if the catalyst caused the XLPE structure cleavage, resulting in a reduction in torque.)

The rheological properties of resulting melt obtained by kneading without and with catalyst were further determined by measuring the dependence of shear viscosity on a shear rate on a high-pressure capillary rheometer. The XLPE flow curves thus obtained are shown in Fig. 5.

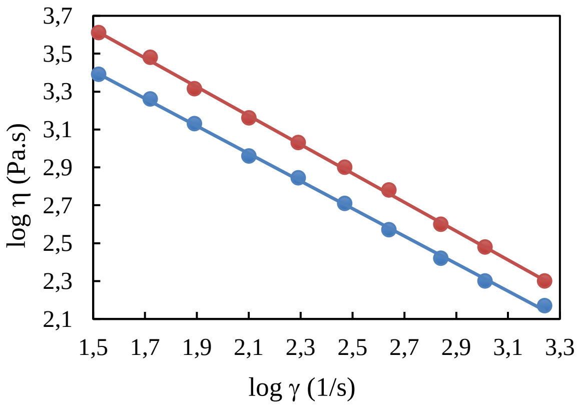

**Fig. 5.** Dependence of shear viscosity of waste XLPE melt (η/Pa.s) on the shear rate ($\gamma$/s$^{-1}$) at 250 °C. Flow curves: upper (red) line – XLPE without catalyst, bottom (blue) line – XLPE with 1% of Ru.

It is evident that over the entire range of shear rate, the shear-viscosity values are significantly lower in the case of incorporated catalyst (blue line), which is in good agreement with the decrease in torque. Overall, above-mentioned findings suggest that catalyst used can promote the splitting of chemical structure of XLPE already in the melt phase.

### 3.4. Pyrolysis with silane-grafted XLPE

All the above findings indicate that the decomposition of waste XLPE in the presence and without catalyst must result in a different composition of pyrolysis products. In the silane process, the crosslinks consist of -Si-O-Si- bonds (siloxane crosslinks). So, compounds with this bond are formed during pyrolysis, which must necessarily be reflected in the pyrolysis products. The resulting products are then not only hydrocarbons, but also Si compounds. Therefore, for deeper understanding of degradation of XLPE structure, pyrolysis with silane-grafted XLPE was performed at different final temperatures, and a mass balance was determined analyzing the gas, oil and solid carbonaceous residue (SCR) obtained both without and with catalyst. The results show Tables 2, 3, 4 and 5.

#### *3.4.1 Mass balance of pyrolysis*

The results obtained allowed to determine the mass balance of the slow pyrolysis process at final temperatures of 450–480 °C for pyrolysis with and without catalyst. The results are summarized in Table 2.

**Tab. 2** Mass balance of pyrolysis of waste silane grafted XLPE (wt.%) without and with catalyst at final temperatures 450–480 °C, delay of 30 min and the heating rate of 5 K min$^{-1}$. SCR – solid carbonaceous residue

| $T_{final}$ (°C) | 450 | 460 | 470 | 480 |
|---|---|---|---|---|
| | Without catalyst | | | |
| Gas | 4.54 | 4.94 | 5.07 | 5.77 |
| Oil | 86.88 | 85.46 | 90.67 | 90.67 |
| SCR | 8.58 | 9.60 | 4.26 | 3.56 |
| | With catalyst | | | |
| Gas | 5.38 | 6.55 | 6.83 | 6.80 |
| Oil | 86.67 | 91.57 | 90.82 | 91.10 |
| SCR | 7.95 | 1.88 | 2.35 | 2.10 |

From the above data it can be concluded that the yields of gas and oil are comparable in both cases, but at the final temperatures above 450 °C, a significantly lower SCR yields were obtained (2 wt.%) with catalyst compared to the yield without catalyst (4–10 wt.%). This fact can play an important role in large-scale pyrolysis, since SCR is clearly a less valuable product (see below). Thus, together with high production of desirable $C_6$–$C_9$ hydrocarbons (see below, Table 4), this is a favorable result of catalysis.

### 3.4.2 Composition of pyrolysis gas

The main components of total pyrolysis gas were light gas hydrocarbons (C1-C5), $CO_2$, and hydrogen (Table 3).

**Tab. 3** Composition of pyrolysis gas obtained without and with Ru/$Al_2O_3$ catalyst (vol.%)

| $T_{final}$ (°C) | 450 | 460 | 470 | 480 |
|---|---|---|---|---|
| Gas | Without catalyst | | | |
| $CH_4$ | 10.9 | 11.9 | 12.5 | 12.2 |
| $C_2$–$C_5$ | 64.2 | 67.1 | 66.1 | 65.2 |
| CO | 3.1 | 2.1 | 2.5 | 1.9 |
| $CO_2$ | 2.1 | 1.8 | 1.6 | 1.6 |
| $H_2$ | 19.7 | 17.1 | 17.2 | 19.2 |
| | With catalyst | | | |
| $CH_4$ | 9.7 | 9.4 | 9.2 | 9.7 |
| $C_2$–$C_5$ | 46.9 | 46.3 | 45.9 | 50.9 |
| CO | 2.0 | 3.4 | 4.5 | 2.1 |
| $CO_2$ | 15.2 | 14.0 | 12.6 | 11.9 |
| $H_2$ | 26.2 | 25.9 | 27.8 | 25.0 |

This observation is consistent with simulation results [39]. It is evident from Table 3 that the total gas obtained with Ru/$Al_2O_3$ catalyst showed a significant increase in CO2 and H2 concentrations (at the expense of gaseous hydrocarbons) compared to that obtained without catalyst. This comparison indicates that the catalyst significantly promotes the cleavage of XLPE and leading to gas formation. The source of CO and $CO_2$ is attributed mainly to the decomposition of siloxane cross-links (Si–O–Si), which introduce oxygen into the system. These can originate from oxygen present in the feedstock (elemental analysis indicates ~3 wt.% O), which is likely associated with siloxane groups, and from residual moisture in the Ru/$Al_2O_3$ catalyst (~2 wt.%).

The gas did not contain undesirable components such as hydrogen sulfide or ammonia which is favorable from a practical point of view.

### 3.4.3 Composition of pyrolysis oil

As expected, both liquid ($C_{10}$–$C_{17}$) and dissolved solid ($C_{18}$–$C_{35}$) hydrocarbons were identified in the pyrolysis oils. However, liquid hydrocarbons $C_6$–$C_9$ were detected only in oils obtained with catalyst (Table 4).

A significant and unexpected finding was the presence of cyclic siloxanes, namely hexamethylcyclotrisiloxane and octamethylcyclotetrasiloxane were detected by GC-MS in all pyrolysis oils obtained without catalyst, whereas they were not detected in oils produced with the catalyst. The content of hexamethylcyklotrisiloxane in the oil obtained without catalyst was 0.34–0.57 wt.% and that of octamethylcyklotrisiloxane was 0.10–0.27 wt.% (Table 4). These results suggest that Ru/$Al_2O_3$ promotes the complete scission of siloxane crosslinks, preventing the formation of cyclic siloxanes.

**Tab. 4** Composition of pyrolysis oil obtained without and with Ru/$Al_2O_3$ catalyst (wt.%)

| $T_{final}$ (°C) | Without catalyst | | | |
|---|---|---|---|---|
| | $C_6$–$C_9$ | $C_{10}$–$C_{17}$ | $C_{18}$–$C_{35}$ | $C_6H_{18}O_3Si_3$ / $C_8H_{24}O_4Si_4$ |
| 450 | 0.00 | 90.61 | 9.39 | - |
| 460 | 0.00 | 94.49 | 5.51 | 0.34/0.13 |
| 470 | 0.00 | 69.50 | 30.50 | 0.57/0.27 |
| 480 | 0.00 | 69.78 | 30.22 | 0.37/0.10 |
| | With catalyst | | | |
| | $C_6$–$C_9$ | $C_{10}$–$C_{17}$ | $C_{18}$–$C_{35}$ | $C_6H_{18}O_3Si_3$ / $C_8H_{24}O_4Si_4$ |
| 450 | 37.10 | 57.14 | 5.76 | 0.00 |
| 460 | 39.23 | 52.89 | 7.88 | 0.00 |
| 470 | 19.79 | 64.97 | 15.24 | 0.00 |
| 480 | 11.09 | 38.60 | 50.31 | 0.00 |

It can be concluded that the catalyst promotes the cleavage of the XLPE structure, especially at final temperatures of 450 and 460 °C, which leads to the formation of highly desirable $C_6$–$C_9$ hydrocarbons (up to 39 wt. %, Table 4). This observation is consistent with the increased $CO_2$ formation in the presence of the catalyst, suggesting that siloxane structures are more extensively decomposed.

### 3.4.4 Characterization of solid carbonaceous residue (SCR)

No coke formations were found in the SCR, either in the absence or presence of the catalyst. The *habitus* of SCR clearly indicated an asphalt-like solid without porous texture (Fig. 6). (Note: in FTIR spectrum, did not confirm the presence of polyaromatics or aromatics, typical for coke).

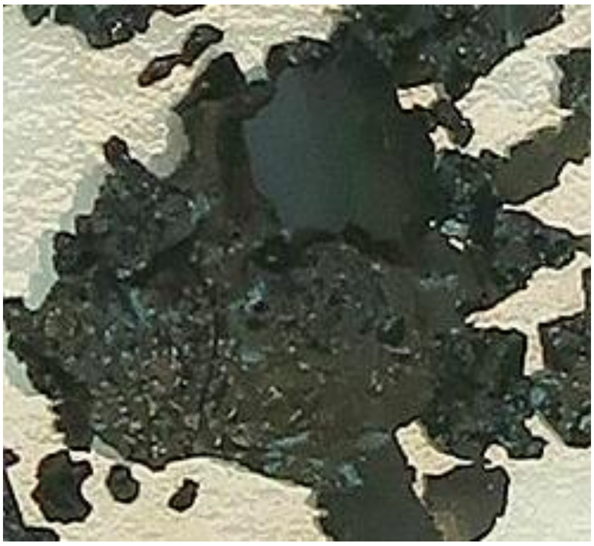

**Fig. 6**. Asphalt-like solid carbonaceous residue.

The resulting SCR was further analyzed by XRF. The most important item was Si (present as $SiO_2$), as its analysis enabled the evaluation of the silicon mass balance in the pyrolysis process. The results are summarized in Table 5, while the Si content in the gas phase was assumed to be zero. Table 5 shows that the input material contained 0.05% Si. In the case of pyrolysis without catalyst, 0.045% Si was found in the obtained oil and 0.006% Si in the obtained SCR, so, giving a total of Si 0.05%, which corresponds to the Si content in the input XLPE. In contrast, for pyrolysis with catalyst, no Si in the obtained oil was detected, whereas the obtained SCR contained 0.05% Si, again corresponding to the initial silicon content.

**Tab. 5** Mass balance of Si (wt.%) for pyrolysis with and without catalyst. SCR – solid carbonaceous residue. Initial XLPE: Si 0.049 ± 0.001 wt.%

| Status | Oil | | |
|---|---|---|---|
| | Si concentration | Yield | Si amount |
| No catalyst | 0.053 ± 0.004 | 85.46 | 0.045 |
| With catalyst | 0.000 | 9.57 | 0.000 |
| | SCR | | |
| | Si concentration | Yield | Si amount |
| No catalyst | 0.062 ± 0.001 | 9.60 | 0.006 |
| With catalyst | 2.766 ± 0.003 | 1.88 | 0.052 |
| | Total | | |
| No catalysts | | | 0.051 |
| With catalyst | | | 0.052 |

Overall, in pyrolysis without catalyst, Si (originally organically bound) was almost completely transferred to the oil phase, while in the case with catalyst, Si (present as $SiO_2$) was completely retained in the SCR. This behavior can be explained by the enhanced cleavage of cross-linked siloxane bonds in the presence of the catalyst.

### *3.4.5 Mass balance of pyrolysis with FCC catalyst*

For comparison with the effect of the widely used catalysts mentioned in the Introduction, the FCC catalyst, which is a well-known cracking zeolite catalyst, was used to degrade the waste silane-grafted XLPE. The FCC catalyst used contained 50% zeolite and pyrolysis was carried out at 470 °C. (For other pyrolysis conditions see Section 2.2.) The mass balance and composition of the key product, oil, were evaluated and compared with those from pyrolysis of XLPE with Ru/$Al_2O_3$. The results are presented in Tables 6 and 7.

Table 6 shows that the cleavage of XLPE structure by slow pyrolysis proceeds differently without catalyst, in the presence of Ru/$Al_2O_3$ and in the presence of FCC catalyst. Pyrolysis without or with Ru/$Al_2O_3$ catalyst gave practically the same oil yield (91 wt.%), but gas was 5 and 7 wt.%, resp., and SCR was 4 and 2 wt.%, respectively.

**Tab. 6** Mass balance of slow pyrolysis of waste silane-grafted XLPE (wt.%) without and with catalysts at the final temperature of 470 °C, delay of 30 min and the heating rate of 5 K $min^{-1}$. SCR – solid carbonaceous residue.

| | Oil | Gas | SCR |
|---|---|---|---|
| Without catalyst | 90.67 | 5.07 | 4.26 |
| With Ru/$Al_2O_3$ (1% Ru) | 90.82 | 6.83 | 2.35 |
| With FCC (1%) | 86.34 | 11.13 | 2.53 |

**Tab. 7** Oil composition from slow pyrolysis of waste silane-grafted XLPE (wt.%) without and with catalysts at the final temperature of 470 °C, delay of 30 min and the heating rate of 5 K $min^{-1}$.

| | C6–C9 | $C_{10}$–$C_{17}$ | $C_{18}$–$C_{35}$ | >$C_{35}$ |
|---|---|---|---|---|
| Without catalyst | 0.00 | 90.61 | 9.39 | 0.00 |
| With Ru/$Al_2O_3$ (1% Ru) | 39.23 | 52.89 | 7.88 | 0.00 |
| With FCC (1%) | 36.74 | 37.46 | 6.19 | 19.61 |

However, pyrolysis without catalyst gave high yield of liquid hydrocarbons (91 wt.%, Table 7), but no significant $C_6$–$C_9$ fraction was found. In the presence of Ru/$Al_2O_3$, a significant proportion of $C_6$–$C_9$ (39 wt.%) was obtained in the oil, as well as a high yield of liquid hydrocarbons.

However, the action of FCC catalyst resulted in a high portion of solid hydrocarbons >$C_{35}$ (20 wt.%, Table 7) at the expense of liquid hydrocarbons (with Ru/$Al_2O_3$, liquid hydrocarbons $C_6$–$C_{17}$ were 92.12 wt.%, those with FCC catalyst only 74.20 wt.%). On the other hand, the long-chain hydrocarbons >$C_{35}$ can be successfully hydrocracked to produce lubricating oils. Slow pyrolysis in the low-temperature range therefore provides several options for obtaining hydrocarbon mixtures. Moreover, at pyrolysis without catalyst, the olefins content in the oil was 31–32 wt.%, with catalyst 44–45 wt.% (determined by GC-MS method). Using the catalyst, significantly more olefins can therefore be produced if necessary.

## 3.5. Description of Ru/$Al_2O_3$ catalyst activity

From the data presented it can be inferred that the crosslink is split to $SiO_2$, $CO_2$ and $H_2$ by the action of higher temperature with promotion of Ru/$Al_2O_3$ catalyst unlike the case without catalyst. This finding can be expressed by the proposed equations (1) and (2):

(1) – without catalyst:

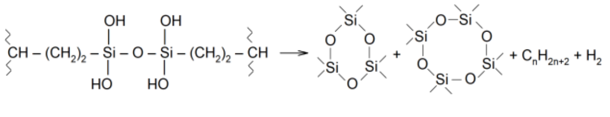

(2) – with catalyst:

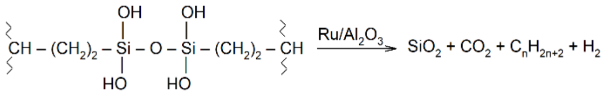

$$\mathrm{CH-(CH_2)_2-\overset{OH}{\underset{HO}{Si}}-O-\overset{OH}{\underset{HO}{Si}}-(CH_2)_2-CH} \xrightarrow{Ru/Al_2O_3} SiO_2 + CO_2 + C_nH_{2n+2} + H_2$$

Equation (1) expresses that scission without catalyst occurs firstly on the ternary carbons of crosslinked structure while hydrocarbons (mainly alkanes) and hydrogen are formed. The split siloxane crosslinks are thermodynamically stabilized by closing into the cyclic structures as clearly evidenced by aforementioned presence of both hexamethylcyclotrisiloxane and octamethylcyclotetrasiloxane in the pyrolysis oils obtained without catalyst. (Table 4).

Equation (2) then express promotion of depolymerization and scission reactions whereby the siloxane crosslinks are completely split by catalyst action to $CO_2$, $H_2$ and $SiO_2$. This is evidenced by (*i*) the mentioned high contents of $CO_2$ and $H_2$ in the total pyrolysis gas (Table 3), (*ii*) absence of hexamethylcyclotrisiloxane and octamethylcyclotetrasiloxane in the pyrolysis oils obtained with Ru/$Al_2O_3$ catalyst (Table 4), (*iii*) by the presence of total Si in the solid pyrolysis residue obtained with catalyst (Table 5).

Overall, the catalyst used significantly promotes the depolymerization and cleavage of XLPE. During the thermal degradation of XPLE, reactions similar to those at the degradation of polyethylenes proceed [40,41,42] (including production of olefins), but they are promoted by the joint action of ruthenium and catalytically strongly acidic sites in $Al_2O_3$. In more detail, $Al_2O_3$ is known to have pronounced Lewis acidic sites [43,44]. However, because the electron configuration of Ru is [Kr] $4d^7$ $5s^1$, Ru contains a vacant d-orbital in a valence shell that is able to accept an electron pair. Due to this, it can act as a Lewis acid, too. Equation (2) can therefore be explained by the joint action of two catalysts with different Lewis acid sites, which can act in different ways. As the result, cleavage and depolymerization of XPLE polymer structure occurs. The contribution of Ru and $Al_2O_3$ to the total catalytic effect is 83% and 17%, respectively, as follows from the fact that at the final temperature 460 °C, with $Al_2O_3$ alone the SCR yield was 9.08 wt.%, but with Ru/$Al_2O_3$ only 1.88 wt.% (Table 2). As 9.08/1.88 = 4.83, it can be inferred that Ru/$Al_2O_3$ is approximately 5 times more effective than $Al_2O_3$ alone, in percentage it is 83% vs. 17%. Another approach to interpreting the cleavage properties of Ru is as follows.

### *3.5.1 The catalytic mechanism of Ru action*

The catalytic mechanism of action of Ru can be (simplistically) described as follows. The +I inductive effect of $CH_2$ groups in the vicinity of tertiary carbons increases the electron density on the tertiary carbons, thus, the tertiary carbons are more reactive compared to secondary ones. In the branched structure of XLPE (see equations (1) and (2)), the tertiary carbons are hydrogen-bonded and surrounded by $CH_2$ groups. These groups tend to give electrons leading to the induction effect. They are less electron-withdrawing than hydrogen, so, they are electron-releasing (electron-donating). This electron-releasing function (indicated by the +I effect) leads to increase of electron density on the tertiary carbon. The increased electron density on the tertiary carbon allows interactions with the Lewis acid site in alumina and vacant d-orbital in a valence shell of Ru. This creates a very unstable complex that decomposes into the described products.

A possible variant of the action of Ru is that the Ru atom has an s-orbital with only one electron in its valence shell. This s-orbital can therefore accept a second electron to complete the maximum number of 2. Thus, the Ru atom can act as a reactive agent and withdraw electrons from the polymer chain, i.e. cleave C–H bonds to form radicals in this way:

$$\begin{aligned} &\mathrm{Ru}\cdot + \mathrm{R{-}CH2{-}R{\sim}} \rightarrow \mathrm{Ru{-}H} + \mathrm{R{-}\dot{C}H{-}R{\sim}} \\ &\rightarrow \mathrm{Ru}\cdot + \mathrm{H}\cdot + \mathrm{R{-}\dot{C}H{-}R{\sim}} \end{aligned} \tag{3}$$

## 3.6. Regeneration of ruthenium catalyst

From a practical point of view, it is important that the Ru/$Al_2O_3$ catalyst can be regenerated by chemical methods [47–50]. However, Ru/$Al_2O_3$ can also be reused directly. This is possible if the catalyst is placed in a layer above the sample, so that it does not mix with the feedstock. Although the catalyst was placed above the sample, it reacts with the volatile decomposition products which pass through the catalytic layer. The reusability of catalyst was tested in this way by pyrolyzing XLPE with the same catalyst 5 times, determining the mass balance of each experiment. If the catalyst was not reusable, the yields of each product would have to change significantly. The result obtained are in Table 8. Since no significant changes in the mass balance were observed, it can be deduced that the possibility of reusing this catalyst is real. This conclusion is based primarily on the small standard deviation of main product, pyrolysis oil, which was only 1%. The standard deviations achieved for the minor products, gas and SCR, 23 and 20%, respectively, can be qualified as acceptable.

**Tab. 8** Mass balance of 5 times repeated pyrolysis of waste XLPE with catalyst (wt.%) at the final temperature of 470 °C, delay of 30 min, the heating rate of 5 K $min^{-1}$. SD – standard deviation

| Item | Gas | Oil | SCR |
|---|---|---|---|
| Average | 6.83 | 90.82 | 2.35 |
| SD | 1.55 | 1.09 | 0.47 |
| | (23%) | (1%) | (20%) |

## 3.7. Outline of possible uses of pyrolysis products

Pyrolysis is generally considered a costly process, in terms of both investment and operation. Therefore, the utilizations of its main products, especially the gas and oil, is of key importance. In this work, only indicative application possibilities based on composition and basic properties are discussed. A detailed evaluation of product utilization and process integration is beyond the scope of this study.

From gas obtained composition (Table 3), the heat content was evaluated as HHV and LHV. The gas obtained without catalyst had HHV 55.44–70.12 MJ $m^{-3}$

and LHV 51.04–64.72 MJ m$^{-3}$. In the case of catalyzed pyrolysis, the heating values were lower HHV 40.41–58.25 MJ m-3, LHV 37.37–53.75 MJ m-3, due to a reduced content of gaseous hydrocarbons in the total gas. Nevertheless, these values remain sufficiently high (for comparison: natural gas has HHV 35.09–45.17 MJ m$^{-3}$ and LHV 31.67–40.84 MJ m$^{-3}$) and allow further use of gas obtained, e.g. in cogeneration units, in gas engines or for heating the waste treatment unit. Such a unit would then be energy efficient or even completely energy self-sufficient.

For the oils obtained (Table 4), the following HHV and LHV values were determined. The HHV ranged 45–51 MJ kg$^{-1}$ and the LHV ranged 42–47 MJ kg$^{-1}$ (Table 9). The oils obtained with and without catalyst showed similar heating values, although at relatively higher final pyrolysis temperatures of 470 and 480 °C, slightly lower values of both LHV and HHV were observed.

**Tab. 9** HHV and LHV of oils obtained without and with catalyst at different final temperatures of pyrolysis

| $T_{final}$ (°C) | HHV (MJ kg$^{-1}$) without catalyst | HHV (MJ kg$^{-1}$) with catalyst |
|---|---|---|
| 450 | 49.74 | 50.63 |
| 460 | 49.95 | 49.27 |
| 470 | 45.31 | 47.11 |
| 480 | 44.63 | 46.52 |
| $T_{final}$ (°C) | LHV (MJ kg$^{-1}$) without catalyst | LHV (MJ kg$^{-1}$) with catalyst |
| 450 | 46.55 | 47.26 |
| 460 | 46.77 | 46.00 |
| 470 | 42.41 | 43.99 |
| 480 | 41.86 | 43.71 |

However, the use of obtained oils as liquid fuels is related to ash, sulfur and nitrogen contents, which must be as low as possible. The proximate and organic elemental analyses showed that the contents of these components were very low to negligible: oils contained no ash, only 0.02–0.04 wt.% of S and 0.02–0.05 wt.% of N. Thus, all oils can be considered practically ash-free, sulfur-free, and nitrogen-free liquids, classifiable as relatively clean fuels. Overall, the oils obtained can be used as a clean liquid fuels or as substitute fuels.

Another possibility of using the obtained oil arises from their physical properties, namely density, viscosity, and fluidity, which were determined at 20 °C. The results are summarized in Table 10 (to assess changes in physical properties, oils obtained at temperatures up to 500 °C were analyzed). The viscosity measurements are intended as a preliminary characterization of the oil properties; however, detailed evaluation for industrial oil applications would require fractionation into defined cuts. It is evident from the values shown that, in the case of oils obtained without catalyst, their dynamic and kinematic viscosity sharply increased at the final pyrolysis temperature above 470 °C, whereas their fluidity rapidly decreased. A similar trend was observed for oils obtained with catalyst; however, the differences between the values were less pronounced. This behavior is likely related to the formation of solid $C_{18}$–$C_{35}$ hydrocarbons by recombination, whose increasing concentration significantly affects the viscosity.

As mentioned, in the case of the oils obtained with catalyst, the differences in the measured properties were less pronounced. This may also be attributed to the formation of $C_6$–$C_9$ liquid hydrocarbons (Table 4).

**Tab. 10** Density (ρ), dynamic viscosity (η), kinematic viscosity (ν) and fluidity (φ) of oils obtained without and with catalyst at different final temperatures of pyrolysis

| $T_{final}$ (°C) | Without catalyst | | | |
|---|---|---|---|---|
| | $\rho$ (kg.m$^{-3}$) | $\eta$ (mPa.s) | $\nu$ (mm$^2$.s$^{-1}$) | $\varphi$ (Pa.s)$^{-1}$ |
| 450 | 794.6 | 3.28 | 4.13 | 304.88 |
| 460 | 795.4 | 2.98 | 3.74 | 335.91 |
| 470 | 797.2 | 4.21 | 5.28 | 237.70 |
| 480 | 801.4 | 141.01 | 175.95 | 7.09 |
| 490 | 804.6 | 136.67 | 169.86 | 7.32 |
| 500 | 806.3 | 157.33 | 195.13 | 6.40 |
| *T*final (°C) | With catalyst | | | |
| | $\rho$ (kg.m$^{-3}$) | $\eta$ (mPa.s) | $\nu$ (mm$^2$.s$^{-1}$) | $\varphi$ (Pa.s)$^{-1}$ |
| 450 | 774.4 | 4.56 | 5.89 | 219.30 |
| 460 | 779.0 | 7.41 | 9.51 | 134.93 |
| 470 | 783.4 | 9.12 | 11.64 | 109.65 |
| 480 | 788.7 | 19.85 | 25.17 | 50.38 |
| 490 | 795.8 | 32.89 | 41.33 | 30.40 |
| 500 | 801.8 | 60.47 | 75.42 | 16.54 |

**Tab. 11** Kinematic viscosity at 40 °C ($\nu_{40}$) of oil obtained without and with catalyst at different final temperatures of pyrolysis

| $T_{final}$ (°C) | $\nu_{40}$ (without catalyst) | $\nu_{40}$ (with catalyst) |
|---|---|---|
| 450 | 4.10 | 5.18 |
| 460 | 3.50 | 5.80 |
| 470 | 4.65 | 7.04 |
| 480 | 61.24 | 11.03 |
| 490 | 58.06 | 18.04 |
| 500 | 70.34 | 28.81 |

Table 11 shows the kinematic viscosity of the oils at 40 °C. This parameter indicates the potential classification of the oils obtained as industrial oils, as these are classified according to the ISO VG viscosity classes based on kinematic viscosity at 40 °C (ISO 3448 [16]). In this case, the oils obtained without catalyst exhibited viscosities of $\nu_{40}$ 3.50–70.34 mm$^2$ s$^{-1}$, corresponding to ISO VG viscosity classes 3, 5 and 68, while oils obtained with catalyst showed viscosities of 5.18–28.21 mm$^2$ s$^{-1}$, corresponding to ISO VG viscosity classes 7, 10 and 32. These classifications suggest potential application areas of use according to ISO 6743 [17]. Thus, the oils obtained can also serve as various oils for further use.

The possibilities of using the oils mentioned above are only outlined here, and their practical application requires further investigation. However, one clear application is the use of oils obtained from catalyzed pyrolysis as solvents and chemicals. It follows from Table 4 that the oils can serve as a source of solvents (high content of $C_6$–$C_9$ hydrocarbons 37–39 wt.% at final temperatures of 450 and 460 °C), liquid hydrocarbons (high content of $C_{10}$–$C_{17}$ hydrocarbons 53–55 wt.% at final temperatures of 450–470 °C), and solid hydrocarbons (content of $C_{18}$–$C_{35}$ hydrocarbons 6–50 wt.% depending on the final temperature of 450–480 °C), especially paraffin. A more detailed evaluation of oil utilization (e.g., fractional distillation and chemical upgrading) is beyond the scope of this study, but the obtained composition suggests its suitability as a feedstock for fuels and petrochemical applications.

As for the minor product, SCR (yield 2–4 wt. %, Table 2), it can be considered a less valued product because, according to a proximate analysis of small amounts obtained, it contains a relatively high amount of ash and shows very low energy content. Therefore, minimizing SCR formation is desirable, which is achieved by using the catalyst.

Overall, the main benefit of catalyzed pyrolysis of waste XLPE is the production of valuable hydrocarbons. Due to the high heating values of the input material (LHV of 43 MJ $kg^{-1}$ and HHV of 46 MJ $kg^{-1}$), this waste can also be used as a solid fuel, however this would result in the permanent loss of valuable hydrocarbon structures.

## 4. Conclusion

The amount of XLPE waste is still growing and needs to be processed. The low-temperature slow Ru/$Al_2O_3$ catalyzed pyrolysis of waste XLPE seems to be a promising way to convert this material into valuable hydrocarbons and energy gas. Therefore, the effects of Ru/$Al_2O_3$ catalyst on the degradation of XLPE structure was investigated and described, and the process conditions were tested.

It was proved that the thermal degradation of XLPE is promoted by Ru/$Al_2O_3$ catalyst which at the same time enables a deep cleavage of rigid XLPE structure. The evidence is that the activation energy of the process is significantly lower in the presence of catalyst compared without catalyst. Further, the torque and shear viscosity values of XLPE melt at 250 °C showed that even small amounts of catalyst used (1 wt.% Ru) promotes the cleavage of XLPE structure already in the melt phase.

Significant results were achieved by slow catalyzed pyrolysis of XLPE up to 470 °C. Analysis of pyrolysis oil as the main product showed that the catalyst used allows for a high content of low $C_6$–$C_9$ hydrocarbons (39 wt.%) and liquid hydrocarbons $C_{10}$–$C_{17}$ (53 wt.%), as well as solid hydrocarbons including paraffin (8 wt.%). Assessment of the physical properties of the oil shows that it can be used as a liquid fuel (LHV 42–47 MJ $kg^{-1}$, HHV 45–51 MJ $kg^{-1}$). Furthermore, the oils obtained without catalyst had kinematic viscosity at 40 °C 3.50–70.34 $mm^2\ s^{-1}$, which classifies them into the ISO VG viscosity classes 3, 5 and 68, and the oils obtained with catalyst 5.18–28.21 $mm^2\ s^{-1}$, which classifies them into the ISO VG viscosity classes 7, 10 and 32. The obtained oils can therefore also serve as industrial oils.

## References

1. M. Selvin, S. Shah, H.J. Maria, S. Thomas, R. Tuladhar, M. Jacob. Review on recycling of cross-linked polyethylene. Ind. Eng. Chem. Res. 63(3) (2024) 1200–1214.
2. H. Ahmad, D. Rodrigue. Crosslinked polyethylene: A review on the crosslinking techniques, manufacturing methods, applications, and recycling. Polym. Eng. Sci. 62(8) (2022) 2376–2401.
3. S. Sen, M.B. Celik. Modeling the effect of plastic oil obtained from XLPE cable waste on diesel engine performance and emission parameters withthe response surface method. Sci. Tech. Energ. Trasition 79 (2024) 58.
4. M. Shan-jun, Z. Jun, L. Dong, Ch. Hong-yin. Study on pyrolysis characteristics of cross-linked polyethylene material cable. Procedia Eng. 52 (2013) 588–592.
5. A. Marcilla, R. Ruiz-Femenia, J. Hernández, J.C. García-Quesada. Thermal and catalytic pyrolysis of crosslinked polyethylene. J. Anal. Appl. Pyrol. 76 (2006) 254–259.
6. S.M. Tamboli, S.T. Mhaske, D.D. Kale. Crosslinked polyethylene. Indian J. Chem. Technol. 11 (2004) 853–864.
7. P. Singh, S. Bhattacharya, et al. Energy recovery from cross-linked polyethylene wastes using pyrolysis and CO2 assisted gasification. Appl. Energy 254 (2019) 113722.
8. T. Naota, H. Takaya, S.-I. Murahashi. Ruthenium-Catalyzed Reactions for Organic Synthesis. Chem. Rev. 98 (1998) 2599−2660.
9. M. Bertoli, A. Choualeb, A.J. Lough, B. Moore, D. Spasyuk,D.G. Gusev. Osmium and Ruthenium Catalysts for Dehydrogenation of Alcohols. Organometallics 30 (2011) 3479–3482.
10. C. Rodrigues, F.G. Delolo, J. Norinder, A. Börner, A.L. Bogado, A.A. Batista. Hydroformylation-hydrogenation and hydroformylation-acetalization
11. 11. P. Straka. A comprehensive study of Power-to-Gas technology: Technical implementations overview, economic assessments, methanation plant as auxiliary operation of lignite-fired power station. J. Clean. Prod. 311 (2021) 127642.
12. S. Ouardad, F. Peruch. Metathetic degradation of trans-1,4-polyisoprene with ruthenium catalysts. Polym. Degrad. Stab. 99 (2014) 249–253.
13. H.B. Kim, E.D. Park. Ammonia decomposition over Ru catalysts supported on alumina with different crystalline phases. Catal. Today 411–412 (2023) 113817.
14. Y. Park, T. Namioka, S. Sakamoto, T.-j. Min, S.-a. Roh, K.Yoshikawa. Optimum operating conditions

for a two-stage gasification process fueled by polypropylene by means of continuous reactor over ruthenium catalyst. Fuel Process. Technol. 91 (2010) 951–957.
15. P. Straka, O. Bičáková, J. Cihlář. Nízkoteplotní zpracování odpadního síťovaného polyethylenu s rutheniobým katalyzátorem. Paliva 15, No.1 (2023) 19–23.
16. J.E. Rorrer, C. Troyano-Valls, G.T. Beckham, Y. Roman-Leshkov. Hydrogenolysis of polypropylene and mixed polyolefin plastic waste over Ru/C to produce liquid alkanes. ACS Sustainable Chem. Eng. 2021, 9, 35, 11661–11666.
17. X. Jia, C. Qin, T. Friedberger, Z. Guan, Z. Huang. Efficient and selective degradation of polyethylenes into liquid fuels and waxes under mild conditions. Sci. Adv. 2 (2016) e1501591.
18. A.S. Goldman, A.H. Roy, Z. Huang, R. Ahuja, W. Schinski, M. Brookhart. Catalytic Alkane Metathesis by Tandem Alkane Dehydrogenation-Olefin Metathesis. Science 312 (2006) 257–261.
19. D. Guironnet and B. Peters. Tandem Catalysts for Polyethylene Upcycling: A Simple Kinetic Model. J. Phys. Chem. A 124 (2020) 3935–3942.
20. N.M. Wang, G. Strong, V. DaSilva, L. Gao, R. Huacuja, I.A. Konstantinov, M.S. Rosen, A.J. Nett, S. Ewart, R. Geyer, S.L. Scott, D. Guironnet. Chemical Recycling of Polyethylene by Tandem Catalytic Conversion to Propylene. J. Am. Chem. Soc. 144 (2022) 18526–18531.
21. V. Farkas, P. Albrecht, B. Csutorás, Á. Erdélyi, M. Nagyházi, G. Turczel, N. Miskolczi, J. Bobek-Nagy, O. Osterthun, J. Klankermayer , R. Tuba. Ruthenium-catalyzed “open-loop” recycling of polyethylene via tandem isomerization-metathesis (ISOMET). Green Chem.26 (2024) 10225–10231.
22. H. Ahmad, D. Rodrigue. Crosslinked polyethylene: A review on the crosslinking techniques, manufacturing methods, applications, and recycling. Polym. Eng. Sci. 62(8) (2022), 2376–2401.
23. E.N. Brown, R.B. Willms, G.T. Gray et al. Influence of Molecular Conformation on the Constitutive Response of Polyethylene: A Comparison of HDPE, UHMWPE, and PEX. Exp. Mech. 47 (2007) 381–393.
24. M. Selvin, S. Shah, H.J. Maria et al. Review on Recycling of Cross-Linked Polyethylene. Ind. Eng. Chem. Res. 63(3) (2024) 1200–1214.
25. M. Fikri, Z. Abdul-Malek. Partial discharge diagnosis and remaining useful lifetime in XLPE extruded power cables under DC voltage: a review. Electr. Eng. 105 (2023) 4195–4212.
26. J. Zhang, J. Li., H. Li, M. Yang, Y. Li, Y. Qi, Y. Xu, W. Hu, B. Liu. Recent Overview and Future Research Prospects of Cross-linked Polyethylene Materials: Cross-linking Methods and Applications. Preprints 2024, 2024091601.
27. L.O. Mark, M.C. Cendejas, I. Hermans, The use of heterogeneous catalysis in the chemical valorization of plastic waste. ChemSusChem 13 (2020) 5808–5836.
28. R. Miandad, M.A. Barakat, A.S. Aburiazaiza, M. Rehan, A.S. Nizami, Catalytic pyrolysis of plastic waste: A review. Process Saf. Environ. 102 (2016) 822–838.
29. H. Ohkita, R. Nishiyama, Y. Tochihara, T. Mizushima, N. Kakuta, Y. Morioka, A. Ueno, Y. Namiki, S. Tanifuji, H. Katoh, H. Sunazuka, R. Nakayama, T. Kuroyanagi. Acid Properties of Silica–Alumina Catalysts and Catalytic Degradation of Polyethylene. Ind. Eng. Chem. Res. 32 (1993) 3112–3116.
30. M.A. Uddin, K. Koizumi, K. Murata, Y. Sakata. Thermal and catalytic degradation of structurally different types of polyethylene into fuel oil. Polym. Degrad. Stabil. 56 (1997) 37–44.
31. Q. Huang, C. Liu, R. Wei, J. Wang. Experimental study of polyethylene pyrolysis and combustion over HZSM-5, HUSY, and MCM-41. J. Hazard Mater. 333 (2017) 10–22.
32. N. Carmo, D. Afonso, E. Santos, I. Fonseca, F. Lemos, M.A.N.D.A. Lemos. Coprocessing of Waste Plastic and Hydrocarbons over MFI (HZSM-5). Int. J. Chem. Kinet. 48 (2016) 329–336.
33. A.L. Figueiredo, A.S. Araujo, M. Linares, A. Peral, R.A. Garcia, D.P. Serrano, V.J. Fernandes. Catalytic cracking of LDPE over nanocrystalline HZSM-5 zeolite prepared by seed-assisted synthesis from an organic-template-free system. J. Anal. Appl. Pyrol. 117 (2016) 132–140.
34. E. Rodriguez, R. Palos, A. Gutierrez, F.J. Vela, J.M. Arandes, J. Bilbao. Effect of the FCC Equilibrium Catalyst Properties and of the Cracking Temperature on the Production of Fuel from HDPE Pyrolysis Waxes. Energ Fuel 33 (2019) 5191–5199.
35. Y. Zhang, D. Duan, H. Lei, E. Villota, R. Ruan. Jet fuel production from waste plastics via catalytic pyrolysis with activated carbons. Appl. Energ. 251 (2019) 113337.
36. S. Colantonio, L. Cafiero, D. De Angelis, N.M. Ipolito, R. Tuffi, S.V. Ciprioti. Thermal and catalytic pyrolysis of a synthetic mixture representative of packaging plastics residue. Front. Chem. Sci. Eng. 14 (2020) 288–303.
37. S.-j. Mo, J. Zhang, D. Liang, H.-y. Chen. Study on pyrolysis characteristics of cross-linked polyethylene material cable. Procedia Engineering 52 (2013) 588–592.
38. P. Atkins, J. de Paula, Reaction dynamics, Thermodynamic aspects. In Physical Chemistry, Ninth Edition; Oxford University Press 2010; p. 849.
39. J. Kong, K. Zhou, X. Ren, Y. Chen, Y. Li, P. Meng. Insight into gaseous product distribution of cross-linked polyethylene pyrolysis using ReaxFF MD simulation and TG-MS. J. Anal. Appl. Pyrol. 169 (2023) 105847.
40. X. Li, N.A. Mahadas, M. Zhang, J. DePodesta, M. Stefik, C. Tang. Sustainable high-density

polyethylene via chemical recycling: From modification to polymerization methods. Polymer 295 (2024) 126698.
41. S. Kumar, A.K. Panda, R.K. Singh. A review on tertiary recycling of high-density polyethylene to fuel. Resour. Conserv. Recycl. 55 (2011) 893–910.
42. A.K. Panda, R.K. Singh, D.K. Mishra. Thermolysis of waste plastics to liquid fuel. A suitable method for plastic waste management and manufacture of value added products – A world prospective. Renew. Sust. Energ. Rev. 14 (2010) 233–248.
43. C.J. Breckner, H.N. Pham, M.G. Dempsey, M.A. Perez-Ahuatl, A.C. Kohl, C.N. Lytle, A.K. Datye, J.T. Miller. The role of Lewis acid in γ-Al2O3 oligomerization. ChemPhysChem 24 (2023) 1–10.
44. T.K. Phung, L.P. Hernández, A. Lagazzo, G. Busca. Dehydration of ethanol over zeolites, silica alumina and alumina: Lewis acidity, Brønsted acidity and confinement effects. Appl. Catal. A Gen. 493 (2015) 77–89.
45. ISO 3448:1992, Industrial liquid lubricants – ISO viscosity classification.
46. ISO 6743-4:2015, Lubricants, industrial oils and related products (class L) – Classification – Part 4: Family H (Hydraulic systems).
47. Patent No. CN101519732A, Method for recycling ruthenium from ruthenium-containing Waste, 2011.
48. Patent No. DE102005061954A1, Recycling of ruthenium from a used ruthenium catalyst comprises treating the catalyst containing ruthenium oxide in a hydrogen stream and treating the carrier material containing ruthenium metal with hydrochloric acid, 2007.
49. Patent No. US4132569A. Ruthenium recovery process, 1979.
50. Patent No. EP0913194A1, Method for reactivating ruthenium catalyst, 2004.